

# Exact integrated completed likelihood maximisation in a stochastic block transition model for dynamic networks

Riccardo Rastelli

riccardo.rastelli@wu.ac.at

Institute for Statistics and Mathematics, WU Vienna University of Economics and Business, Austria.

## Abstract

The latent stochastic block model is a flexible statistical model which is widely used for the analysis of network data. Extensions of this model to a dynamic context often fail to capture the persistence of edges in contiguous network snapshots. The recently introduced stochastic block transition model addresses precisely this issue, by modelling the probabilities of creating a new edge and of maintaining an edge over time. Using a model-based clustering approach, this paper illustrates a methodology to fit stochastic block transition models under a Bayesian framework. The method relies on a greedy optimisation procedure to maximise the exact integrated completed likelihood. The computational efficiency of the algorithm used makes the methodology scalable and appropriate for the analysis of large network datasets. Crucially, the optimal number of latent groups is automatically selected at no additional computing cost. The efficacy of the method is demonstrated through applications to both artificial and real datasets.

**Keywords:** Stochastic Block Transition Models, Dynamic Networks, Greedy Optimisation, Integrated Completed Likelihood, Clustering.

## 1 Introduction

Research on networks has gained an incredible momentum in the last few decades. In fact, networks can be used to represent observed phenomena in a variety of research areas, including social sciences, epidemiology, biology, earth sciences, technology and finance. Social networks, such as collaboration networks or proximity networks, are largely available, and they pose stimulating research challenges since they typically require the design of scalable computational methods.

Most frequently, network data is provided in the form of an adjacency matrix, where each entry  $x_{ij}$  characterises the interaction between the nodes  $i$  and  $j$ . The Stochastic

Block Model (SBM), as characterised by Wang and Wong (1987), is a flexible statistical model that can be used to analyse large social networks. In the SBM, the nodes of the network are assigned to latent groups based on their connection preferences: two nodes belonging to the same group are said stochastically equivalent, meaning that they have the same probability of connecting to any other node in the network. This concept generalises the idea of community structure (see Fortunato (2010) and references therein), since disassortative behaviours may be represented. The SBM framework effectively defines a clustering problem, where one has to estimate from the data both the nodes' cluster membership variables (*allocations*) and the underlying number of clusters. This may be tackled in a number of ways, including sampling based approaches (Nowicki and Snijders 2001), or optimisation approaches relying on the Expectation-Maximisation algorithm (Daudin et al. 2008). A recent survey on SBMs can be found in Matias and Robin (2014).

Other celebrated networks models that are often used in the analysis of social networks are the Exponential Random Graph Model of Wasserman and Pattison (1996), the Latent Position Model of Hoff et al. (2002), and other types of latent variable models, such as the Mixed Membership SBM of Airoldi et al. (2008).

The network models mentioned so far are usually called *static*, since they can only model a single adjacency matrix which does not possess a time dimension. By contrast, in the vast majority of cases, the observed interactions are (in some way) dynamically evolving over time. This implies that static network models can only be used after the data has been aggregated into a single matrix, causing a loss of information. This limitation has prompted new directions in research, with a special focus on new statistical models for *dynamic* networks, i.e. networks evolving over time. A useful survey on some of the work on this topic can be found in Holme and Saramäki (2012).

Most dynamic network models are conceived as extensions of the aforementioned static frameworks. Regarding the SBM, one interesting approach considers the interactions as instantaneous events which may be observed repeatedly in any time interval. Matias et al. (2015) and Corneli et al. (2017) model these interactions as realised events of a non-homogeneous Poisson point process, where the intensity parameters are determined by the cluster memberships of the corresponding nodes.

A more substantial part of the literature consists instead of approaches that rely on a discretisation of the time dimension, which leads to a collection of adjacency matrices

indexed according to their ordering in time. Most works following this approach typically introduce a Markov property that creates a temporal dependence between any two contiguous network snapshots. For example, Yang et al. (2011) assume a hidden Markov model where the hidden states are the cluster membership variables of the nodes. The network snapshots are all marginally dependent, but they become independent conditionally on the hidden states. In other words, the temporal dependency is captured only through the evolution of the latent allocation variables over time. By contrast, Xu and Hero (2014) model instead the time dependency only through a state-space model on the connection probabilities between the SBM blocks. Matias and Miele (2017) consider a more general framework that includes the previous two as special cases, proving that identifiability of these Markovian models may be lost if both cluster membership variables and connectivity parameters are allowed to change over time. They also propose an estimation method that can handle networks with non-binary interactions. Rastelli et al. (2017) propose instead a Bayesian framework for the same model, focusing on the computational efficiency and scalability of the inferential process. Other relevant dynamic extensions of the SBM are introduced in Ishiguro et al. (2010) and Bartolucci et al. (2015).

As concerns the other static network models, a number of extensions have been also proposed in recent years. Examples include Hanneke et al. (2010) for the Temporal Exponential Random Graph Model; Sarkar and Moore (2005) and Sewell and Chen (2015) for dynamic Latent Position Models; and finally Xing et al. (2010) and Ho et al. (2011) for evolving Mixed Membership SBMs. Similarly to the literature on temporal SBMs, these works introduce hidden processes to explain the temporal dependence of the network snapshots.

In many cases, however, the observed dynamic networks tend to be particularly stable, or, equivalently, they exhibit a strong temporal dependency. This may have important repercussions, since it ultimately questions whether the temporal dynamics of the models are necessary, or if the static frameworks may be just as effective. Xu (2015) addresses exactly this issue, proposing an original model that builds upon a dynamic SBM to include a Markov property on the observed edge values. Differently from the SBM structure, this model is specifically designed for temporal networks, and it clusters the nodes in each time frame according to their propensity to create new edges and maintaining existing ones. Since it directly models the transitions of the edge values, it is called the Stochastic

Block Transition Model (SBTM). In the SBTM, the probability of observing an edge depends on whether the same edge was present or absent in the previous time frame, creating a direct dependence between any two contiguous network snapshots. Xu (2015) gives evidence that the SBTM can successfully model the creation and the duration of the interactions, hence being much more flexible than the dynamic SBM of Xu and Hero (2014).

Although in different contexts, other works propose similar modelling ideas: Friel et al. (2016) consider an extension of the Latent Position Model for bipartite dynamic networks, and they introduce additional parameters to explicitly capture the persistence of edges over time. Zhang et al. (2016), instead, study a model similar to the SBTM, obtained through a discretisation of an underlying continuous-time process. They consider a framework that facilitates both the theoretical characterisation of such model and a likelihood-based inferential procedure. Finally, Heaukulani and Ghahramani (2013) propose a type of block model where the evolution over time of the latent allocation of each node is affected by the cluster memberships of its neighbours.

This paper focuses on the SBTM. First, a new Bayesian hierarchical structure for this model is introduced, following the same ideas as in Rastelli et al. (2017). Then, the modelling assumptions are exploited to analytically integrate out (*collapse*) most of the model parameters, as also advocated by Nobile and Fearnside (2007), McDaid et al. (2013), and Côme and Latouche (2015). This collapsing leads to an exact formula for the well known Integrated Completed Likelihood (ICL), which is widely used as an optimality criterion in the statistical analysis of finite mixtures (Biernacki et al. 2000). The exact ICL value obtained is maximised with respect to the allocation variables using a heuristic greedy procedure, which resembles the algorithms described by Côme and Latouche (2015), Wyse et al. (2017), and Rastelli et al. (2017). A crucial advantage of the methodology proposed is that the number of latent groups can be automatically deduced from the allocation variables at any stage of the optimisation. In addition, the approach can deal with subjects leaving the study (temporarily or permanently) by including a special group of inactive nodes. The algorithm takes full advantage of this information, which allows the method to be very computationally efficient and scalable, as illustrated in the application.

The methodology is tested on artificially generated networks, showing that it achieves good convergence properties and overall good clustering performance. A human contact

dataset is used to give a demonstration of the procedure, showing that the results obtained are also very easy to interpret.

Finally, the R package `GreedySBTM` accompanies this paper and it provides an implementation of the algorithm described. The package is publicly available on CRAN (R Core Team 2017).

The paper is organised as follows: Sections 2 and 3 illustrate the Bayesian SBTM, Sections 4 and 5 describe the exact ICL approach and the optimisation algorithm, and finally the methodology is applied to simulated and a real dataset in Sections 6 and 7, respectively.

## 2 The Stochastic Block Transition Model

The statistical model used in this paper is a variation of that introduced by Xu (2015). The differences between the two models are minor and do not affect the principle ideas that motivate the use of the SBTM; nonetheless they are necessary to give integrity to the inferential procedure used in this paper. A more detailed account of the modifications and a comparison with other statistical models for dynamic network data is provided at the end of the next section.

The observed data consist of a collection of  $T$  graphs, where the edges of each of these represent interactions between the corresponding nodes at different times. In each time frame  $t = \{1, \dots, T\}$ , some of the nodes may be *inactive*, in which case none of their edge values are observed, or they simply do not have any interaction. The data may be described through two binary cubes  $\mathcal{X}$  and  $\mathcal{Y}$  of size  $N \times N \times T$ , which are characterised by:

$$y_{ij}^{(t)} = \begin{cases} 1 & \text{if both nodes } i \text{ and } j \text{ are active at time frame } t, \\ 0 & \text{otherwise;} \end{cases} \quad (1)$$

$$x_{ij}^{(t)} = \begin{cases} 1 & \text{if } y_{ij}^{(t)} = 1 \text{ and an edge between } i \text{ and } j \text{ appears at time } t, \\ 0 & \text{if } y_{ij}^{(t)} = 0 \text{ or no edge appears between } i \text{ and } j \text{ at time } t, \end{cases} \quad (2)$$

for all  $i$  and  $j$  in  $\{1, \dots, N\}$  and  $t$  in  $\{1, \dots, T\}$ . Evidently,  $\mathcal{Y}$  simply serves as an activity indicator, whereas  $\mathcal{X} = \{\mathbf{X}^{(1)}, \dots, \mathbf{X}^{(T)}\}$  corresponds to a collection of canonical adjacency matrices for the observed edge values. The  $T$  graphs are assumed to be undirected and without self-edges, hence each of the adjacency matrices is symmetric and has zeros on the diagonal.

In the SBTM, a clustering structure is hypothesised on the nodes of the  $T$  observed graphs. Each of the nodes, at each time frame, is characterised by a cluster membership variable taking values in the discrete set  $\{0, 1, \dots, K\}$ . The notation  $\mathcal{Z} = \left\{ z_i^{(t)} : i = 1, \dots, N, t = 1, \dots, T \right\}$  is used to denote all such allocations. Also, the equivalent notation  $z_{ig}^{(t)} = \mathbb{1}(\{z_i^{(t)} = g\})$  may be used in some equations ( $\mathbb{1}$  denotes the indicator function). Note that the vector  $\mathbf{z}^{(t)} = \left\{ z_1^{(t)}, \dots, z_N^{(t)} \right\}$  denotes a partition of  $\{1, \dots, N\}$ , for every  $t$ . Finally, the label zero is reserved for inactive nodes, i.e.  $z_i^{(t)} = 0$  iff  $i$  is inactive at time  $t$ : since the inactive nodes are known, there is no interest in inferring these allocations and hence they are kept fixed throughout.

The probability that the observed edge indexed by  $(i, j, t)$  takes value 1 is defined as:

$$\begin{aligned} \rho_{ij}^{(t)} &= \mathbb{P} \left( x_{ij}^{(t)} = 1 \mid y_{ij}^{(t)} = 1, y_{ij}^{(t-1)}, x_{ij}^{(t-1)}, z_i^{(t)} = g, z_j^{(t)} = h, \theta_{gh}, P_{gh}, Q_{gh} \right) \\ &= 1 - \mathbb{P} \left( x_{ij}^{(t)} = 0 \mid y_{ij}^{(t)} = 1, y_{ij}^{(t-1)}, x_{ij}^{(t-1)}, z_i^{(t)} = g, z_j^{(t)} = h, \theta_{gh}, P_{gh}, Q_{gh} \right) \\ &= \begin{cases} \theta_{gh} & \text{if } y_{ij}^{(t-1)} = 0 \\ P_{gh} & \text{if } y_{ij}^{(t-1)} = 1 \text{ and } x_{ij}^{(t-1)} = 0 \\ 1 - Q_{gh} & \text{if } y_{ij}^{(t-1)} = 1 \text{ and } x_{ij}^{(t-1)} = 1. \end{cases} \end{aligned} \quad (3)$$

Note that if  $t = 1$  then  $y_{ij}^{(t-1)} = 0$  for all  $i$  and  $j$ . The probability of an edge  $\rho_{ij}^{(t)}$  is defined by (3) only if  $y_{ij}^{(t)} = 1$ , in fact, only observed edges may contribute to the likelihood value. Equation (3) essentially characterises the alternation of three regimes:

- A SBM-type of connection probability  $\theta_{gh}$  is selected whenever there is no information regarding the previous value of the edge considered.
- A SBTM probability  $P_{gh}$  is used when it is known that the edge considered had value zero in the previous time frame. The value  $P_{gh}$  corresponds to the probability of creating a new edge.
- A SBTM probability  $Q_{gh}$  is used when it is known that the edge considered had value one in the previous time frame. The probability of confirming the edge is  $1 - Q_{gh}$ , hence  $Q_{gh}$  may be interpreted as the probability of destroying an existing edge.

These parameters  $\{\theta_{gh}\}_{g,h}$ ,  $\{P_{gh}\}_{g,h}$  and  $\{Q_{gh}\}_{g,h}$  form the matrices  $\Theta$ ,  $\mathbf{P}$  and  $\mathbf{Q}$  respectively, which contain the edge probabilities for nodes belonging to any two given groups.

The full likelihood of the model can be written as:

$$\mathcal{L}_{\mathcal{X}, \mathcal{Y}}(\mathcal{Z}, \Theta, \mathbf{P}, \mathbf{Q}) = \prod_{t=1}^T \prod_{i < j} \left\{ \left[ p_{ij}^{(t)} \right]^{x_{ij}^{(t)}} \left[ 1 - p_{ij}^{(t)} \right]^{1 - x_{ij}^{(t)}} \right\}^{y_{ij}^{(t)}} \quad (4)$$

which is simply a product of contributions given by Bernoulli variables. Hereafter, the product  $\prod_{i<j}$  stands for  $\prod_{i=1}^{N-1} \prod_{j=i+1}^N$ , for brevity. The likelihood function may be reformulated in a more convenient way, taking advantage of the block structure and hence grouping up the terms in (4). In order to do this, the following quantities are needed, for all  $g$  and  $h$  in  $\{1, \dots, K\}$ :

$$\eta_{gh} = \sum_{i<j} y_{ij}^{(1)} x_{ij}^{(1)} \lambda_{ij1gh} + \sum_{t>1} \sum_{i<j} y_{ij}^{(t)} \left(1 - y_{ij}^{(t-1)}\right) x_{ij}^{(t)} \lambda_{ijtgh}; \quad (5)$$

$$\zeta_{gh} = \sum_{i<j} y_{ij}^{(1)} \left(1 - x_{ij}^{(1)}\right) \lambda_{ijtgh} + \sum_{t>1} \sum_{i<j} y_{ij}^{(t)} \left(1 - y_{ij}^{(t-1)}\right) \left(1 - x_{ij}^{(1)}\right) \lambda_{ijtgh}; \quad (6)$$

$$U_{gh}^{uv} = \sum_{t>1} \sum_{i<j} y_{ij}^{(t)} y_{ij}^{(t-1)} \left[1 - \left(u - x_{ij}^{(t-1)}\right)^2\right] \left[1 - \left(v - x_{ij}^{(t)}\right)^2\right] \lambda_{ijtgh}; \quad (7)$$

$$\begin{aligned} \lambda_{ijtgh} &= z_{ig}^{(t)} z_{jh}^{(t)} + z_{ih}^{(t)} z_{jg}^{(t)} - z_{ig}^{(t)} z_{jg}^{(t)} z_{ih}^{(t)} z_{jh}^{(t)} \\ &= \begin{cases} 1 & \text{if } (i, j, t) \text{ refers to an edge between groups } g \text{ and } h; \\ 0 & \text{otherwise.} \end{cases} \end{aligned} \quad (8)$$

The values  $u$  and  $v$  are in  $\{0, 1\}$ . Also note that for binary values  $c_1$  and  $c_2$ :

$$1 - (c_1 - c_2)^2 = \begin{cases} 1 & \text{if } c_1 = c_2; \\ 0 & \text{otherwise.} \end{cases} \quad (9)$$

The quantities introduced in (5), (6) and (7) are crucial summaries of the data. They can be interpreted as the number of successes in creating a SBM-edge ( $\eta_{gh}$ ), in creating a new edge ( $U_{gh}^{01}$ ), and destroying an existing edge ( $U_{gh}^{10}$ ), between a node in group  $g$  and one in group  $h$ . Similarly,  $\zeta_{gh}$ ,  $U_{gh}^{00}$  and  $U_{gh}^{11}$  correspond to the number of failures for the same events, respectively. Using these new quantities, the likelihood function factorises as follows:

$$\mathcal{L}_{\mathcal{X}, \mathcal{Y}}(\mathcal{Z}, \Theta, \mathbf{P}, \mathbf{Q}) = \prod_{g=1}^K \prod_{h=g}^K \theta_{gh}^{\eta_{gh}} (1 - \theta_{gh})^{\zeta_{gh}} P_{gh}^{U_{gh}^{01}} (1 - P_{gh})^{U_{gh}^{00}} Q_{gh}^{U_{gh}^{11}} (1 - Q_{gh})^{U_{gh}^{10}}. \quad (10)$$

This likelihood formulation is particularly similar to those proposed in Xu (2015) and Zhang et al. (2016). Exactly as in SBMs, the presence of blocks simplifies the model structure, and can be exploited to design efficient inferential procedures.

### 3 Bayesian hierarchical structure

The modelling assumptions used in this paper resemble those used in Rastelli et al. (2017). The prior distributions described in this section are all conjugate, and, as a special case,

they permit a non-informative framework which may be used to nullify the subjective contribution induced by the user.

As concerns the allocations, these are assumed to evolve according to  $N$  independent Markov chains on the states  $\{0, \dots, K\}$ . The processes share the same transition probability matrix  $\mathbf{\Pi}$ , which is hence characterised by:

$$\pi_{gh} = \mathbb{P} \left( z_i^{(t)} = h \mid z_i^{(t-1)} = g \right), \quad (11)$$

for all  $i = 1, \dots, N$  and  $t = 2, \dots, T$ . The initial states are assumed to be drawn from a categorical distribution with probabilities  $\alpha_0, \dots, \alpha_K$  proportional to the aggregated group sizes:

$$\alpha_g \propto \sum_{t=2}^T \sum_{i=1}^N z_{ig}^{(t)}. \quad (12)$$

These group proportions approximate the probabilities of the stationary distribution of the Markov chain. Hence, the prior probability of a set of allocations  $\mathcal{Z}$  may be written as follows:

$$\begin{aligned} \mathbb{P}(\mathcal{Z} | \mathbf{\Pi}) &= \mathbb{P}(\mathbf{z}^{(1)} | \boldsymbol{\alpha}) \prod_{t=2}^T \mathbb{P}(\mathbf{z}^{(t)} | \mathbf{z}^{(t-1)}, \mathbf{\Pi}) \\ &= \prod_{g=0}^K [\alpha_g]^{N_g^{(1)}} \prod_{g=0}^K \prod_{h=0}^K [\pi_{gh}]^{R_{gh}}, \end{aligned} \quad (13)$$

where  $N_g^{(t)} = \sum_{i=1}^N z_{ig}^{(t)}$  and  $R_{gh} = \sum_{t=2}^T \sum_{i=1}^N z_{ig}^{(t-1)} z_{ih}^{(t)}$ , for all  $t, i$  and  $g$ . Note that, while inactive nodes do not give any contribution to the likelihood in (4), their group membership affects the prior distribution at all times. In fact, the transition probability matrix  $\mathbf{\Pi}$  has size  $(K+1) \times (K+1)$ , and it includes the probabilities for a node to be activated or inactivated. The rows of the transition probability matrix  $\mathbf{\Pi}$  are assumed to be independent realisations of Dirichlet random vectors:

$$(\pi_{g0}, \dots, \pi_{gK}) \sim Dir(\delta_{g0}, \dots, \delta_{gK}), \quad (14)$$

with  $\delta_{gh}$  being a user-defined hyperparameter, for all  $gs$  and  $hs$ .

As concerns the likelihood parameters, the entries of the matrices  $\boldsymbol{\Theta}$ ,  $\mathbf{P}$  and  $\mathbf{Q}$  all correspond to the success probabilities of Bernoulli random variables: for this reason, independent Beta priors are adopted:

$$\begin{aligned} \theta_{gh} &\sim Beta(\eta_{gh}^0, \zeta_{gh}^0); \\ P_{gh} &\sim Beta(a_{gh}^{\mathbf{P}}, b_{gh}^{\mathbf{P}}); \\ Q_{gh} &\sim Beta(a_{gh}^{\mathbf{Q}}, b_{gh}^{\mathbf{Q}}). \end{aligned} \quad (15)$$

The complete set of hyperparameters is  $\phi = \left\{ \delta_{gh}, \eta_{gh}, \zeta_{gh}, a_{gh}^{\mathbf{P}}, b_{gh}^{\mathbf{P}}, a_{gh}^{\mathbf{Q}}, b_{gh}^{\mathbf{Q}} \right\}_{g,h}$ . These values should be set so that the corresponding prior distributions describe the prior knowledge available on the model parameters. In this paper, non-informative Jeffreys' priors are assumed throughout on all model parameters: this is achieved by setting all the components of  $\phi$  to 0.5.

A graphical representation of the dependencies in the model is shown in Figure 1.

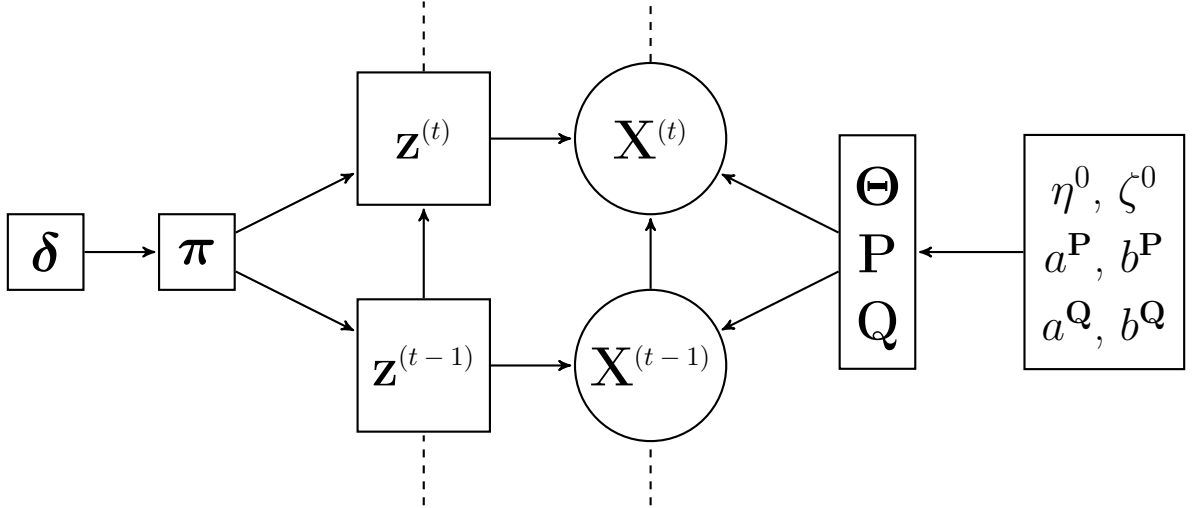


Figure 1: Graphical model for the SBTM described.

The Bayesian hierarchical structure proposed in this section extends the model proposed by Xu (2015). In particular, here the allocations are allowed to change according to a Markov process, following the approaches of Matias and Miele (2017) and Rastelli et al. (2017). This specification creates an additional temporal dependence, and it ultimately permits an assessment of the stability of the network. The same feature also distinguishes this model from that of Zhang et al. (2016), where the allocations do not change over time.

Another important difference with the work of Xu (2015) is the absence of the scaling factors. Here, the matrices  $\mathbf{P}$ , and  $\mathbf{Q}$  do not change over time, so, the additional factors, which ensure that connection probabilities are comparable across different time frames, are in fact not necessary.

## 4 Exact Integrated Completed Likelihood

The Integrated Completed Likelihood (ICL), first introduced in Biernacki et al. (2000), is a model-based clustering criterion used to estimate the number of clusters in finite mixture models. In the dynamic network context addressed in this paper, the exact ICL corresponds to the following value:

$$\mathcal{ICL}_{ex} = \mathbb{P}(\mathcal{X}, \mathcal{Y}, \mathcal{Z} | \phi, K). \quad (16)$$

Since the data  $(\mathcal{X}, \mathcal{Y})$  is fixed, the  $\mathcal{ICL}_{ex}$  index is also equivalent to the marginal posterior for the allocations:

$$\mathcal{ICL}_{ex} \propto \mathbb{P}(\mathcal{Z} | \mathcal{X}, \mathcal{Y}, \phi, K). \quad (17)$$

In other words, the  $\mathcal{ICL}_{ex}$  value can be obtained by analytically integrating out all of the model parameters from the full posterior distribution  $\pi(\mathcal{Z}, \Theta, \mathbf{P}, \mathbf{Q}, \mathbf{\Pi} | \mathcal{X}, \mathcal{Y}, \phi, K)$ . In fact, thanks to the conjugacy of the prior distributions, such integration is analytically possible, and the exact ICL results as follows:

$$\begin{aligned} \mathcal{ICL}_{ex} \propto & \prod_{g=0}^K \left\{ [\alpha_g]^{N_g^1} \cdot \frac{\Gamma\left(\sum_{h=0}^K \delta_{gh}\right)}{\Gamma\left(\sum_{h=0}^K \delta_{gh} + \sum_{h=0}^K R_{gh}\right)} \prod_{h=0}^K \frac{\Gamma(\delta_{gh} + R_{gh})}{\Gamma(\delta_{gh})} \right\} \\ & \cdot \prod_{g=1}^K \prod_{h=g}^K \left\{ \frac{\Gamma(\eta_{gh}^0 + \zeta_{gh}^0)}{\Gamma(\eta_{gh}^0) \Gamma(\zeta_{gh}^0)} \cdot \frac{\Gamma(\eta_{gh}^0 + \eta_{gh}) \Gamma(\zeta_{gh}^0 + \zeta_{gh})}{\Gamma(\eta_{gh}^0 + \eta_{gh} + \zeta_{gh}^0 + \zeta_{gh})} \right\} \\ & \cdot \prod_{g=1}^K \prod_{h=g}^K \left\{ \frac{\Gamma(a_{gh}^{\mathbf{P}} + b_{gh}^{\mathbf{P}})}{\Gamma(a_{gh}^{\mathbf{P}}) \Gamma(b_{gh}^{\mathbf{P}})} \cdot \frac{\Gamma(a_{gh}^{\mathbf{P}} + U_{gh}^{01}) \Gamma(b_{gh}^{\mathbf{P}} + U_{gh}^{00})}{\Gamma(a_{gh}^{\mathbf{P}} + U_{gh}^{01} + b_{gh}^{\mathbf{P}} + U_{gh}^{00})} \right\} \\ & \cdot \prod_{g=1}^K \prod_{h=g}^K \left\{ \frac{\Gamma(a_{gh}^{\mathbf{Q}} + b_{gh}^{\mathbf{Q}})}{\Gamma(a_{gh}^{\mathbf{Q}}) \Gamma(b_{gh}^{\mathbf{Q}})} \cdot \frac{\Gamma(a_{gh}^{\mathbf{Q}} + U_{gh}^{10}) \Gamma(b_{gh}^{\mathbf{Q}} + U_{gh}^{11})}{\Gamma(a_{gh}^{\mathbf{Q}} + U_{gh}^{10} + b_{gh}^{\mathbf{Q}} + U_{gh}^{11})} \right\}. \end{aligned} \quad (18)$$

## 5 Greedy optimisation

The only unknown quantities in (17) and (18) are the allocations  $\mathcal{Z}$ . In fact, for a given clustering configuration  $\mathcal{Z}$ , the corresponding value of  $K$  may be automatically deduced by counting the number of non empty groups. Hence, an optimisation problem can be set up to find the allocations  $\hat{\mathcal{Z}}$  maximising  $\log(\mathcal{ICL}_{ex})$ , by searching in the space of all possible clustering configurations.

This discrete optimisation problem is known to be NP-hard, and it can be solved exactly only through enumeration, which is impractical even for very small datasets.

However, heuristic greedy algorithms have been shown to perform well in similar types of clustering problems: the procedure proposed here follows the same ideas as in Karrer and Newman (2011), Côme and Latouche (2015), Bertolotti et al. (2015), and Rastelli et al. (2017).

First, a maximum number of groups allowed, denoted  $K_{up}$ , is fixed. For small datasets this may be set to  $NT$ , however, for larger networks, a smaller value may be chosen to reduce the computing time. Then, an initial clustering configuration with  $K_{up}$  groups is generated. This may be created at random, or following initialisation methods based on the k-means algorithm, such as those described in Matias and Miele (2017) or Rastelli et al. (2017). At this point the main routine of the algorithm starts, where an active node  $(t, i)$  is selected, and its allocation is updated. For the update, all possible moves to group  $1, \dots, K_{up}$  are tested, and, finally, the change yielding the best increase in the objective function is performed (note that the label zero remains exclusive of inactive nodes throughout). This process continues in a loop until no further increase is possible. After convergence, hierarchical clustering updates are attempted on the final solution obtained, following exactly the same procedure described in Côme and Latouche (2015) and Rastelli et al. (2017). The computing time demanded by this last step is usually negligible, yet it may improve the final solution by merging together some of the groups. The pseudocode for the algorithm (called **GreedyICL**) is provided in Algorithm 1. Note that, in the pseudocode,  $\ell_{(t,i) \rightarrow \hat{g}}$  denotes the value corresponding to the current allocations with node  $(t, i)$  moved to group  $g$ .

Both **GreedyICL** and the final merge procedure only involve greedy updates, so they can only increase the objective function value. However, there is no guarantee that the final solution will correspond to a global optimum of  $\log(\mathcal{ICL}_{ex})$ : for this reason, several restarts of the whole procedure may be beneficial to avoid local optima.

From the algorithmic point of view, one main advantage of these greedy updates is their scalability: the increase in the objective function for each move can be evaluated very efficiently. Furthermore, convergence is usually reached after very few updates of each of the allocations. More detailed explanations regarding the computational savings are provided for example in Côme and Latouche (2015) and Rastelli et al. (2017) and references therein.

As already pointed out, the number of groups can be deduced from the allocation variables at any stage. This makes **GreedyICL** particularly appealing, because, in one

---

**Algorithm 1 GreedyICL**

---

Set  $K_{up}$  and initialise the allocations  $\mathcal{Z}$ .  
Evaluate the objective function and set  $\ell = \ell_{stop} = \log(\mathcal{ICL}_{ex})$ .  
Set  $stop = false$ .  
**while**  $!stop$  **do**  
  Set  $\mathcal{U} = \{(t, i) : z_i^{(t)} \neq 0, t = 1, \dots, T, i = 1, \dots, N\}$ .  
  Shuffle the elements of  $\mathcal{U}$ .  
  **while**  $\mathcal{U}$  is not empty **do**  
     $(t, i) = pop(\mathcal{U})$ .  
     $\hat{g} = \arg \max_{g=1,2,\dots,K_{up}} \ell_{(t,i) \rightarrow g}$ .  
     $\ell = \ell_{(t,i) \rightarrow \hat{g}}$ .  
     $z_i^{(t)} = \hat{g}$ .  
  **end while**  
  **if**  $\ell \leq \ell_{stop}$  **then**  $stop = true$  **else**  $\ell_{stop} = \ell$ .  
  **end if**  
**end while**  
Return  $\mathcal{Z}$  and  $\ell$ .

---

single algorithmic framework, it can return an estimate of the best  $K$ , according to the exact ICL criterion. Currently there are no other works that give any indication on how the number of groups of a SBTM may be inferred from the data. In fact, the GreedyICL methods advocated by Bertolotti et al. (2015), Côme and Latouche (2015), Wyse et al. (2017), and Rastelli et al. (2017) are the only model-based clustering procedures that do not rely on a grid search over all possible  $K$  values, which becomes impractical if the number of groups is large.

## 6 Simulations

In this Section, artificial data is used to validate the methodology described in this paper. The number of time frames considered is  $T = 20$ , whereas two scenarios are possible for the number of nodes:  $N = 50$  or  $N = 250$ . The artificial networks are generated using the hierarchical structure described in Section 3, with  $K = 3$  and the hyperparameters all set to 0.5. This means that the networks are generated through the same posterior distribution which is being optimised, with only  $K$  being arbitrarily fixed. 100 networks are independently generated, and the methodology described in Section 5 is run on each of them, once for each  $K_{up}$  in  $\{10, 20, 30\}$ . Figure 2 shows the objective function values

for the true allocations and for the estimated clustering after each of the steps of the optimisation. For most datasets, and for both small and large networks, the final solution

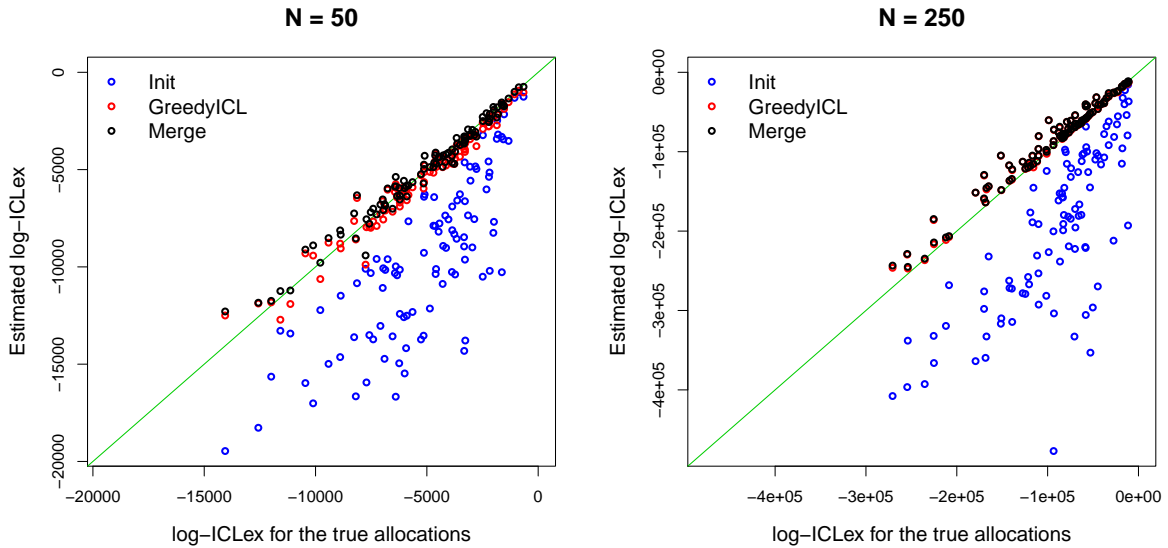


Figure 2: **Simulation study.**  $\log(\mathcal{ICL}_{ex})$  values for the true allocations (on the horizontal axes) and for the best estimated clustering across all  $K_{up}$  values (on the vertical axes). The blue circles correspond to the values obtained after the initialisation using  $k$ -means, the red circles to those obtained after the **GreedyICL** described in 1 and the black circles correspond to the values obtained at the end of the merging procedure.

achieves better  $\log(\mathcal{ICL}_{ex})$  values than the true clustering, suggesting good convergence. Also, the increase granted by the **GreedyICL** step is generally much larger than that given by the final merge step.

Figure 3 focuses instead on the performance of the  $\mathcal{ICL}_{ex}$  criterion. The Normalised Information Criterion (Strehl and Ghosh 2002) is used to compare each estimated partition to its corresponding true counterpart. The plot on the left panel of Figure 3 shows a very high level of agreement, particularly for the larger datasets. Note that this criterion is normalised, hence it should not be affected by the value of  $N$ .

Regarding the optimal number of groups (shown on the right panel of Figure 3), it seems that the criterion tends towards an overestimation, at least in larger networks. This may be related to the presence of more outliers which increase the heterogeneity of the data. Finally, both plots highlight that the choice of  $K_{up}$  does not affect performance. Note that a smaller  $K_{up}$  reduces the computing time, yet the optimal partition can only be found if  $K_{up}$  is greater than the optimal number of groups. Hence, in general, the higher  $K_{up}$  the better; nevertheless, smaller  $K_{up}$  values may be used to speed up the

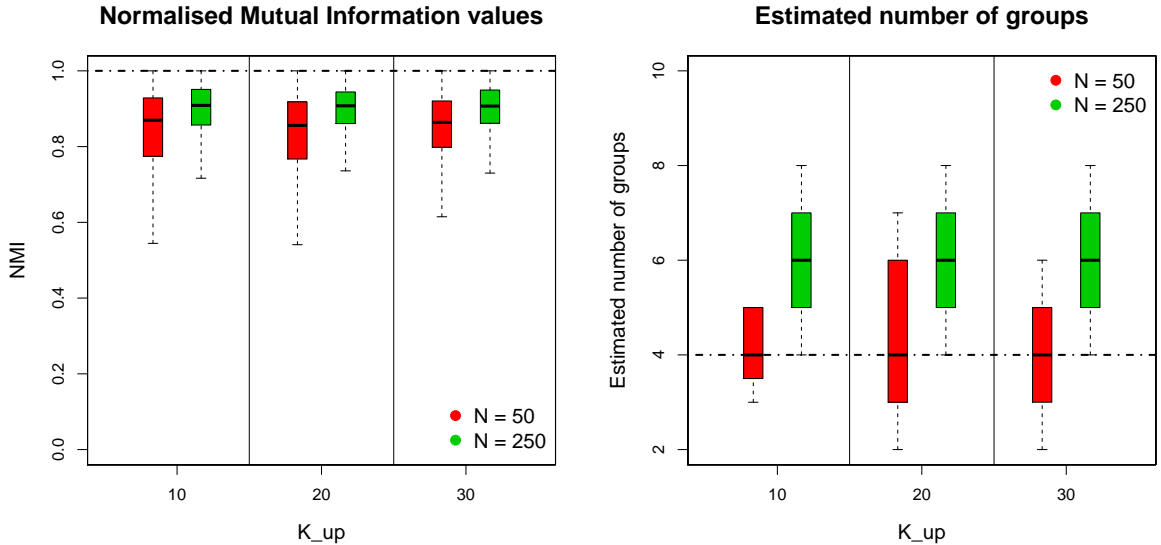


Figure 3: **Simulation study.** The left panel shows the Normalised Mutual Information index between the true clustering and the estimated clustering, for all combinations of  $K_{up}$  and  $N$ . The boxplots represent the values across all generated networks and time frames (the index is in fact evaluated for each  $t = \{1, \dots, T\}$  independently). The boxplots on the right panel are generated in the same way, and they show the estimated number of groups at each time frame.

algorithm or to force it to return a solution with fewer groups.

## 7 Reality Mining dataset

The Reality Mining experiment was performed in 2004 as part of the Reality Commons project. The data was collected and first described by Eagle and Pentland (2006), and it includes human contacts between Massachusetts Institute of Technology (MIT) students, from 14 September 2004 to 5 May 2005. KONECT (the Koblenz Network Collection) provides a public version of a proximity network extracted from the Reality Mining data. The dataset describes proximity interactions of students through a list of undirected edges and their corresponding time stamp. The number of nodes having at least one interaction is  $N = 96$ , and the total number of interactions is 1,086,404. The 9 months were discretised in  $T = 1392$  time frames of 4 hours each. Then, an adjacency cube  $\mathcal{X}$  of size  $N \times N \times T$  was created as follows:

$$x_{ij}^{(t)} = \begin{cases} 1 & \text{if nodes } i \text{ and } j \text{ had at least one interaction between } t - 1 \text{ and } t, \\ 0 & \text{otherwise.} \end{cases} \quad (19)$$

The distribution of edges in the new representation is shown in Figure 4. The nodes were considered inactive in all of the time frames where they had zero interactions: overall,

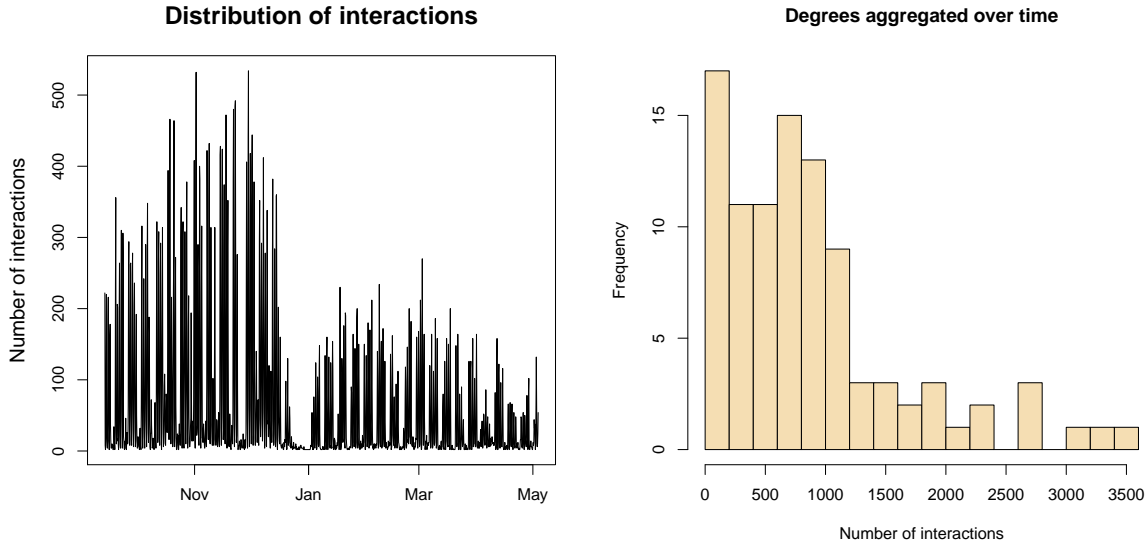


Figure 4: **Reality mining dataset.** The plot on the left panel shows the number of edges at each of the time frames. The plot on the right panel shows instead the frequencies for the total number of edges incident to each node.

approximately 83% of the allocation variables were set to zero. The algorithm was then run with  $K_{up} = 20$  and it converged after 15 iterations and 115 seconds.

The resulting number of groups is  $K = 5$ , meaning that if a node is active, it will select one of 5 different connectivity profiles at each time frame. The sizes of the groups of active nodes aggregated over time are  $N_1 = 10,143$ ,  $N_2 = 5,940$ ,  $N_3 = 2,095$ ,  $N_4 = 4,315$ , and  $N_5 = 547$ . Figure 5 shows the frequencies of the number of groups across all of the time frames. The plots suggest that very often several of the groups are empty, meaning that the network is temporarily homogeneous. This is emphasised in Figure 6, where the size of all groups is shown for each time frame. The migrations between groups exhibit a clear temporal pattern, mostly following the day/night cycle. Additionally, a longer period of inactivity is observed at the end of December, where most nodes become inactive.

Plug-in estimators for the connection probabilities are available as follows:

$$\hat{P}_{gh} = \frac{U_{gh}^{01}}{U_{gh}^{01} + U_{gh}^{00}}; \quad \hat{Q}_{gh} = \frac{U_{gh}^{10}}{U_{gh}^{10} + U_{gh}^{11}}; \quad \hat{\theta}_{gh} = \frac{\eta_{gh}}{\eta_{gh} + \zeta_{gh}}; \quad \hat{\pi}_{gh} = \frac{R_{gh}}{\sum_{h=0}^K R_{gh}}. \quad (20)$$

For the Reality Mining dataset considered, these quantities are shown in Figure 7 through the matrices  $\hat{\mathbf{P}}$ ,  $\hat{\mathbf{Q}}$ ,  $\hat{\mathbf{\Theta}}$  and  $\hat{\mathbf{\Pi}}$ , respectively. The matrices  $\hat{\mathbf{\Theta}}$  and  $\hat{\mathbf{P}}$  exhibit high values on the leading diagonal suggesting assortative behaviour and the presence of community structure. The matrix  $\hat{\mathbf{Q}}$  exhibits the opposite situation, suggesting that edges are destroyed more frequently only if the nodes do not belong to the same group. This is

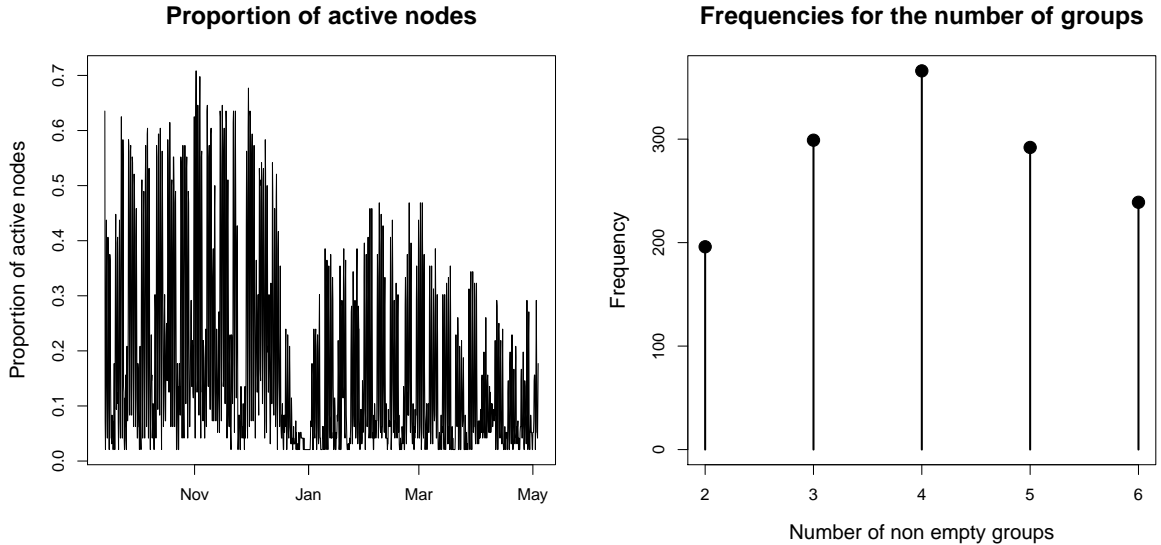


Figure 5: *Reality mining dataset.* The plot on the left panel shows the proportion of nodes which are active in each time frame. The plot on the right panel shows instead the number of time frames where the number of non empty groups is equal to  $k$ , for  $k = 1, \dots, 6$ .

reasonable, since it implies that edges between nodes in the same group are created more frequently and kept for a longer time, confirming the presence of communities.

The matrix  $\hat{\Pi}$  exhibits high values on the diagonal which suggests high stability, since nodes tend not to change much their allocations over time. This is particularly true for group zero, containing the inactive nodes, which also continuously attracts nodes from all other groups.

## 8 Conclusions

This paper has introduced a new methodology to estimate the number of groups and the optimal clustering of the nodes of a Stochastic Block Transition Model. The criterion optimised is the exact Integrated Completed Likelihood, which has recently also been adopted in several other network models. Such criterion is maximised using an iterative greedy procedure, which is known to be particularly computationally efficient. In addition, the method infers the number of latent groups within the same algorithmic framework, hence without requiring a grid search over all possible models.

The procedure has been applied to both artificial and real dataset, showing that it can scale well with the size of the data. The simulation study has shown that the method usually converges to excellent solutions, yet in larger datasets it may overestimate the

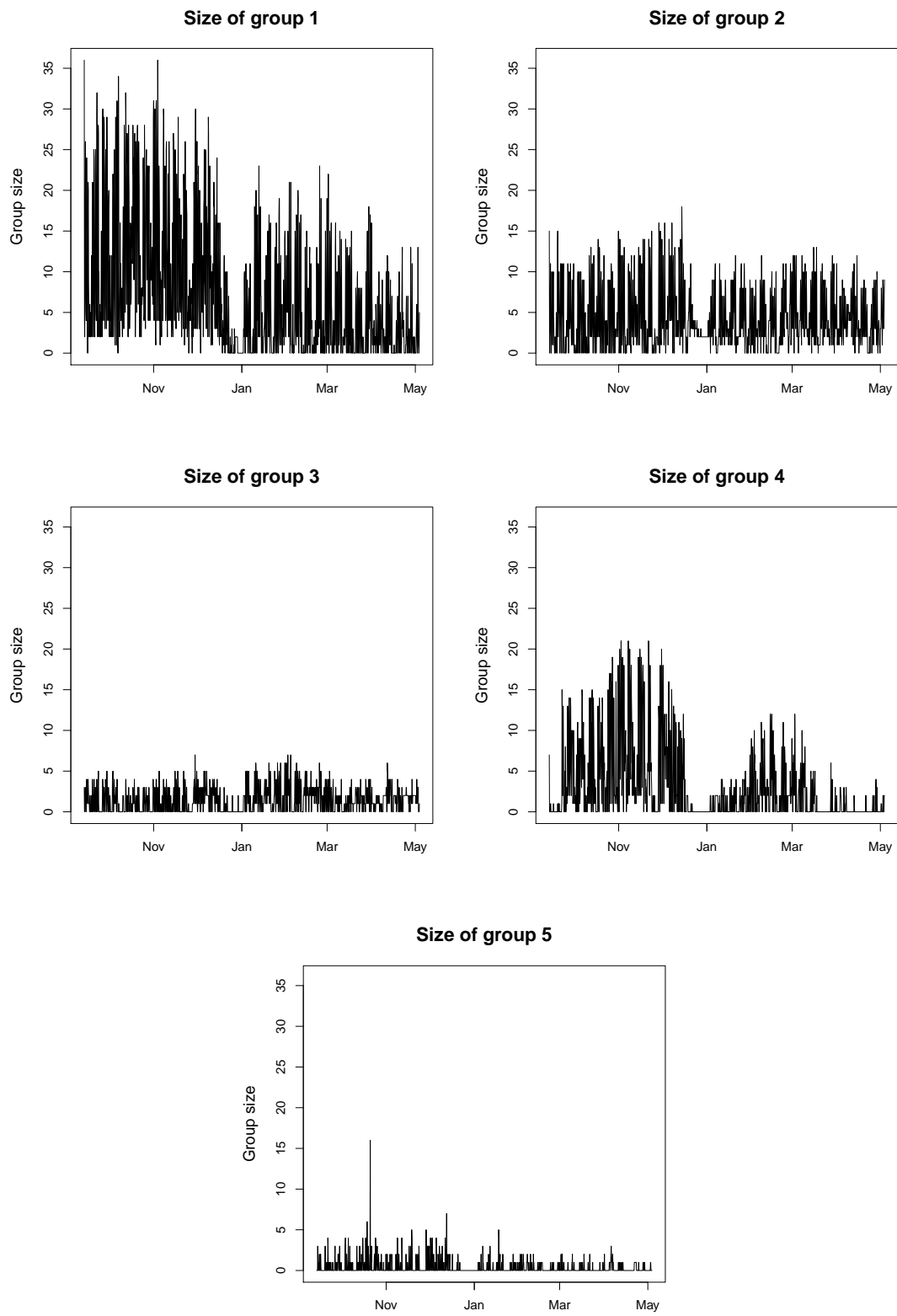


Figure 6: *Reality mining dataset*. These plots show the number of nodes contained by each group at every time frame.

	$\hat{P}$	$\hat{Q}$																																																															
	<table border="1" style="border-collapse: collapse; width: 100%;"> <tr><td>0.04</td><td>0.05</td><td>0.04</td><td>0.01</td><td>0.16</td></tr> <tr><td>0.05</td><td>0.39</td><td>0.13</td><td>0.01</td><td>0.22</td></tr> <tr><td>0.04</td><td>0.13</td><td>0.36</td><td>0</td><td>0.61</td></tr> <tr><td>0.01</td><td>0.01</td><td>0</td><td>0.34</td><td>0</td></tr> <tr><td>0.16</td><td>0.22</td><td>0.61</td><td>0</td><td>0.77</td></tr> </table>	0.04	0.05	0.04	0.01	0.16	0.05	0.39	0.13	0.01	0.22	0.04	0.13	0.36	0	0.61	0.01	0.01	0	0.34	0	0.16	0.22	0.61	0	0.77	<table border="1" style="border-collapse: collapse; width: 100%;"> <tr><td>0.38</td><td>0.61</td><td>0.75</td><td>0.69</td><td>0.42</td></tr> <tr><td>0.61</td><td>0.17</td><td>0.66</td><td>0.65</td><td>0.52</td></tr> <tr><td>0.75</td><td>0.66</td><td>0.07</td><td>0.98</td><td>0.19</td></tr> <tr><td>0.69</td><td>0.65</td><td>0.98</td><td>0.33</td><td>0.9</td></tr> <tr><td>0.42</td><td>0.52</td><td>0.19</td><td>0.9</td><td>0.08</td></tr> </table>	0.38	0.61	0.75	0.69	0.42	0.61	0.17	0.66	0.65	0.52	0.75	0.66	0.07	0.98	0.19	0.69	0.65	0.98	0.33	0.9	0.42	0.52	0.19	0.9	0.08													
0.04	0.05	0.04	0.01	0.16																																																													
0.05	0.39	0.13	0.01	0.22																																																													
0.04	0.13	0.36	0	0.61																																																													
0.01	0.01	0	0.34	0																																																													
0.16	0.22	0.61	0	0.77																																																													
0.38	0.61	0.75	0.69	0.42																																																													
0.61	0.17	0.66	0.65	0.52																																																													
0.75	0.66	0.07	0.98	0.19																																																													
0.69	0.65	0.98	0.33	0.9																																																													
0.42	0.52	0.19	0.9	0.08																																																													
	$\hat{\Theta}$	$\hat{\Pi}$																																																															
	<table border="1" style="border-collapse: collapse; width: 100%;"> <tr><td>0.07</td><td>0.07</td><td>0.04</td><td>0.01</td><td>0.22</td></tr> <tr><td>0.07</td><td>0.57</td><td>0.12</td><td>0.01</td><td>0.21</td></tr> <tr><td>0.04</td><td>0.12</td><td>0.75</td><td>0</td><td>0.64</td></tr> <tr><td>0.01</td><td>0.01</td><td>0</td><td>0.34</td><td>0</td></tr> <tr><td>0.22</td><td>0.21</td><td>0.64</td><td>0</td><td>0.58</td></tr> </table>	0.07	0.07	0.04	0.01	0.22	0.07	0.57	0.12	0.01	0.21	0.04	0.12	0.75	0	0.64	0.01	0.01	0	0.34	0	0.22	0.21	0.64	0	0.58	<table border="1" style="border-collapse: collapse; width: 100%;"> <tr><td>0.92</td><td>0.04</td><td>0.02</td><td>0.01</td><td>0.02</td><td>0</td></tr> <tr><td>0.44</td><td>0.53</td><td>0.01</td><td>0</td><td>0</td><td>0.02</td></tr> <tr><td>0.27</td><td>0.04</td><td>0.68</td><td>0</td><td>0.01</td><td>0</td></tr> <tr><td>0.29</td><td>0.02</td><td>0.01</td><td>0.68</td><td>0</td><td>0</td></tr> <tr><td>0.37</td><td>0.03</td><td>0.01</td><td>0</td><td>0.6</td><td>0</td></tr> <tr><td>0.21</td><td>0.44</td><td>0.01</td><td>0</td><td>0</td><td>0.32</td></tr> </table>	0.92	0.04	0.02	0.01	0.02	0	0.44	0.53	0.01	0	0	0.02	0.27	0.04	0.68	0	0.01	0	0.29	0.02	0.01	0.68	0	0	0.37	0.03	0.01	0	0.6	0	0.21	0.44	0.01	0	0	0.32		
0.07	0.07	0.04	0.01	0.22																																																													
0.07	0.57	0.12	0.01	0.21																																																													
0.04	0.12	0.75	0	0.64																																																													
0.01	0.01	0	0.34	0																																																													
0.22	0.21	0.64	0	0.58																																																													
0.92	0.04	0.02	0.01	0.02	0																																																												
0.44	0.53	0.01	0	0	0.02																																																												
0.27	0.04	0.68	0	0.01	0																																																												
0.29	0.02	0.01	0.68	0	0																																																												
0.37	0.03	0.01	0	0.6	0																																																												
0.21	0.44	0.01	0	0	0.32																																																												

Figure 7: **Reality mining dataset:** Estimated connection and transition probability matrices. The values for the group of inactive nodes are included only in  $\hat{\Pi}$ , in the bottom-right corner.

number of groups. This seems to be a weak spot for the exact ICL criterion itself, since similar issues may be argued in other related works, such as Rastelli et al. (2017).

The application to the Reality Mining dataset offers a demonstration of the results that can be obtained. In this dataset, intense interaction periods appear to be distinctly fragmented due to recurring intervals of inactivity. The modelling approach proposed in this paper can handle this scenario in a natural way, and, more importantly, it can exploit the presence of inactive nodes to mitigate the computational burden.

This paper has focused on binary dynamic networks only. It may be interesting to extend this approach to the non-binary case, and to find a way to model the transitions on the edge values that allow for computationally efficient inferential procedures. Also, the discretisation of the time dimension may have a non-negligible effect on the data analysis: this is for example highlighted in Matias et al. (2015). Hence, another important future step would be to extend the Stochastic Block Transition Model principle to networks that

evolve continuously on time.

Regarding the inferential procedure, several alternatives may be considered: similarly to Matias and Miele (2017), a variational Expectation-Maximisation algorithm may be employed to find the latent clustering and the model parameters within the same algorithmic framework; or, following the approaches of Wyse and Friel (2012), McDaid et al. (2013), and White et al. (2016), a collapsed Gibbs sampler may be used to sample the allocations from their marginal posterior distribution, hence obtaining an assessment of the uncertainty regarding both clustering and number of groups.

The R package **GreedySBTM** accompanies this paper: it contains a C++ implementation of the algorithms described in Section 5, and it includes the adapted version of the Reality Mining dataset used in Section 7. The package is publicly available on CRAN (R Core Team 2017).

## Acknowledgements

The author thanks Kevin Xu for the useful conversations. This research was supported through the Vienna Science and Technology Fund (WWTF) Project MA14-031.

## References

- Airoldi, E. M., D. M. Blei, S. E. Fienberg, and E. P. Xing (2008). “Mixed membership stochastic blockmodels”. In: *Journal of Machine Learning Research* 9, pp. 1981–2014.
- Bartolucci, F., M. F. Marino, and S. Pandolfi (2015). “Composite likelihood inference for hidden Markov models for dynamic networks”. In:
- Bertoletti, M., N. Friel, and R. Rastelli (2015). “Choosing the number of clusters in a finite mixture model using an exact integrated completed likelihood criterion”. In: *Metron* 73.2, pp. 177–199.
- Biernacki, C., G. Celeux, and G. Govaert (2000). “Assessing a mixture model for clustering with the integrated completed likelihood”. In: *Pattern Analysis and Machine Intelligence, IEEE Transactions on* 22.7, pp. 719–725.
- Côme, E. and P. Latouche (2015). “Model selection and clustering in stochastic block models based on the exact integrated complete data likelihood”. In: *Statistical Modelling*, p. 1471082X15577017.
- Corneli, M., P. Latouche, and F. Rossi (2017). “Multiple change points detection and clustering in dynamic network”. In: *HAL-preprint*.
- Daudin, J. J., F. Picard, and S. Robin (2008). “A mixture model for random graphs”. In: *Statistics and Computing* 18.2, pp. 173–183.
- Eagle, N. and A. S. Pentland (2006). “Reality mining: sensing complex social systems”. In: *Personal and ubiquitous computing* 10.4, pp. 255–268.

- Fortunato, S. (2010). “Community detection in graphs”. In: *Physics reports* 486.3, pp. 75–174.
- Friel, N., R. Rastelli, J. Wyse, and A. E. Raftery (2016). “Interlocking directorates in Irish companies using a latent space model for bipartite networks”. In: *Proceedings of the National Academy of Sciences* 113.24, pp. 6629–6634.
- Hanneke, S., W. Fu, and E. P. Xing (2010). “Discrete temporal models of social networks”. In: *Electronic Journal of Statistics* 4, pp. 585–605.
- Heaukulani, C. and Z. Ghahramani (2013). “Dynamic probabilistic models for latent feature propagation in social networks”. In: *International Conference on Machine Learning*, pp. 275–283.
- Ho, Q., L. Song, and E. P. Xing (2011). “Evolving cluster mixed-membership blockmodel for time-evolving networks”. In: *International Conference on Artificial Intelligence and Statistics*, pp. 342–350.
- Hoff, P. D., A. E. Raftery, and M. S. Handcock (2002). “Latent space approaches to social network analysis”. In: *Journal of the American Statistical Association* 97.460, pp. 1090–1098.
- Holme, P. and J. Saramäki (2012). “Temporal networks”. In: *Physics reports* 519.3, pp. 97–125.
- Ishiguro, K., T. Iwata, N. Ueda, and J. B. Tenenbaum (2010). “Dynamic infinite relational model for time-varying relational data analysis”. In: *Advances in Neural Information Processing Systems*, pp. 919–927.
- Karrer, B. and M. E. J. Newman (2011). “Stochastic blockmodels and community structure in networks”. In: *Physical Review E* 83.1, p. 016107.
- Matias, C. and V. Miele (2017). “Statistical clustering of temporal networks through a dynamic stochastic block model”. In: *Journal of the Royal Statistical Society: Series B (Statistical Methodology)* 79.4, pp. 1119–1141.
- Matias, C. and S. Robin (2014). “Modeling heterogeneity in random graphs through latent space models: a selective review”. In: *ESAIM: Proceedings and Surveys* 47, pp. 55–74.
- Matias, C., T. Rebafka, and F. Villers (2015). “A semiparametric extension of the stochastic block model for longitudinal networks”. In: *arXiv preprint arXiv:1512.07075*.
- McDaid, A. F., T. B. Murphy, N. Friel, and N. J. Hurley (2013). “Improved Bayesian inference for the stochastic block model with application to large networks”. In: *Computational Statistics & Data Analysis* 60, pp. 12–31.
- Nobile, A. and A. T. Fearnside (2007). “Bayesian finite mixtures with an unknown number of components: the allocation sampler”. In: *Statistics and Computing* 17.2, pp. 147–162.
- Nowicki, K. and T. A. B. Snijders (2001). “Estimation and prediction for stochastic blockstructures”. In: *Journal of the American Statistical Association* 96.455, pp. 1077–1087.
- R Core Team (2017). *R: A Language and Environment for Statistical Computing*. R Foundation for Statistical Computing. Vienna, Austria. URL: <https://www.R-project.org/>.
- Rastelli, R., P. Latouche, and N. Friel (2017). “Choosing the number of groups in a latent stochastic block model for dynamic networks”. In: *arXiv preprint arXiv:1702.01418*.
- Sarkar, P. and A. W. Moore (2005). “Dynamic social network analysis using latent space models”. In: *SIGKDD Explorations: Special Edition on Link Mining* 7, pp. 31–40.

- Sewell, D. K. and Y. Chen (2015). “Latent space models for dynamic networks”. In: *Journal of the American Statistical Association* 110.512, pp. 1646–1657.
- Strehl, A. and J. Ghosh (2002). “Cluster ensembles—a knowledge reuse framework for combining multiple partitions”. In: *Journal of machine learning research* 3.Dec, pp. 583–617.
- Wang, Y. J. and G. Y. Wong (1987). “Stochastic blockmodels for directed graphs”. In: *Journal of the American Statistical Association* 82, pp. 8–19.
- Wasserman, S. and P. Pattison (1996). “Logit models and logistic regressions for social networks: I. An introduction to Markov graphs and  $p^*$ ”. In: *Psychometrika* 61.3, pp. 401–425.
- White, A., J. Wyse, and T. B. Murphy (2016). “Bayesian variable selection for latent class analysis using a collapsed Gibbs sampler”. In: *Statistics and Computing* 26.1-2, pp. 511–527.
- Wyse, J. and N. Friel (2012). “Block clustering with collapsed latent block models”. In: *Statistics and Computing* 22.2, pp. 415–428.
- Wyse, J., N. Friel, and P. Latouche (2017). “Inferring structure in bipartite networks using the latent block model and exact ICL”. In: *Network Science (to appear)*.
- Xing, Eric P., Wenjie Fu, and Le Song (2010). “A state-space mixed membership block-model for dynamic network tomography”. In: *Ann. Appl. Stat.* 4.2, pp. 535–566. DOI: 10.1214/09-AOAS311.
- Xu, K. (2015). “Stochastic block transition models for dynamic networks”. In: *Artificial Intelligence and Statistics*, pp. 1079–1087.
- Xu, K. S. and A. O. Hero (2014). “Dynamic stochastic blockmodels for time-evolving social networks”. In: *Selected Topics in Signal Processing, IEEE Journal of* 8.4, pp. 552–562.
- Yang, T., Y. Chi, S. Zhu, Y. Gong, and R. Jin (2011). “Detecting communities and their evolutions in dynamic social networks – a Bayesian approach”. In: *Machine learning* 82.2, pp. 157–189.
- Zhang, X., C. Moore, and M. E. J. Newman (2016). “Random graph models for dynamic networks”. In: *arXiv preprint arXiv:1607.07570*.